Genetic Algorithms Applied to the Aerodynamic Design of Transonic Airfoils

Domenico Quagliarella*
Centro Italiano Ricerche Aerospaziali, Capua, Italy 81043
and
Antonio Della Cioppa†
Consiglio Nazionale delle Ricerche, Napoli, Italy 80131

Nomenclature

Cd_w = wave drag coefficient
Cl = lift coefficient
Cp = pressure coefficient
f_k = generic modification function
M = Mach number
t = thickness-to-chord ratio
t_c = assigned airfoil maximum thickness
t_y = computed airfoil maximum thickness
y = airfoil ordinate
y_b = base airfoil ordinate
y_{te} = trailing-edge thickness
w_k = weight of modification function f_k
α = angle of attack

Introduction

THIS work focuses on the application of genetic algorithms to the design of shockless transonic airfoils. The genetic algorithm selects a number of airfoils from a population by means of the fitness function related to the airfoil performance, and then it applies a mixture of crossover and random mutation operators over the selected individuals to generate a new population. The process is iterated until convergence criteria are met.

Genetic algorithms offer an effective answer to complex optimization problems as they are able to effectively explore a very large space of potential solutions.

Successful applications to complex design problems in the aerospace field can be found in Refs. 1–3.

Genetic Algorithms and Optimization

Genetic algorithms can be defined as a general and domain independent optimization and search technique that emulates the mechanisms of selection and mutation of natural evolution. The behavior of a genetic algorithm can be specified by defining some basic string operators (selection, crossover, mutation) and their interactions.[4] The fundamental characteristic of such a class of algorithms is that they do not work directly on the problem variables but on a "string" representation called chromosome.

A population of such strings evolves under the action of selection, mutation, and crossover operators.

The selection mechanism relies on the evaluation of the adaptive value (fitness) that each individual expresses in the assigned environment.[5]

The fitness values are used to select the population members that will mate.

The selection mechanism here chosen is the remainder stochastic sampling without replacement.[4] The mating mechanism chosen is the one-point crossover. Given a couple of strings, a crossover point is randomly selected and a new couple of strings is obtained swapping the genetic material.

Afterward, the obtained strings pass through a mutation. This process consists of a random variation of a small portion of the information coded in the strings.

It is usually convenient to keep the mutation probability low, while, on the other hand, the crossover should apply to a large part of the string population. In the present application, a few population members, the best two, were directly copied into the new generation, while the remaining ones were built using crossover and mutation.

The airfoil is represented using a linear combination of a baseline shape and some given modification functions:

$$y = y_b + \sum_{k=1}^{n} w_k f_k \tag{1}$$

If a constraint on the airfoil maximum thickness is present, then it may be convenient to ensure the automatic satisfaction of such a constraint by scaling the airfoil in the following way:

$$y_c = y(t_c/t_y) \tag{2}$$

The aerodynamic coefficients of each element of the population are evaluated using a full potential flowfield solver.[6] When a population is generated, a decoding procedure builds the airfoils following the instructions stored in the "chromosomes," and then the flowfield solver computes the aerodynamic coefficients that are used to compute the fitness.

Design Examples

Each variable was coded using a seven-bit length substring. Twenty-eight parameters were used to modify the airfoil shape, and the length of the coding string was, therefore, 196 bits. The grid used for each analysis run had 128 angular divisions and 32 radial divisions. A cambered base airfoil was adopted. The population size is of 30 elements for each run reported here. Each generation but the first therefore requires 28 airfoil evaluations, because the best two elements of each generation are copied in the next.

Single-Point Design

The following design problem for a transonic airfoil has been used to test the algorithm:

$$\begin{cases} \max(Cl^2/Cd_w) \\ \text{subject to: } Cl = 0.855 \\ \qquad\qquad M = 0.745 \\ \qquad\qquad 0.0805 \le t \le 0.085 \\ \qquad\qquad 0.0201 \le y_{te} \le 0.0206 \end{cases} \tag{3}$$

In this case the maximization of the fitness with fixed Cl leads to the wave drag minimization.

The optimization procedure stopped after 70 generations because the stated maximum fitness value was reached. One-thousand nine-hundred sixty-two population elements were examined. Three-hundred eighty-one airfoils were discarded before the aerodynamic analysis because geometric constraints were violated, 1190 airfoils were analyzed with the flowfield solver, while the remaining 391 airfoils had the score assigned without analysis because their representative strings were equal to some other previously examined airfoils. Figure 1 shows base and final airfoils in enlarged scale ordinate axis to highlight the modifications. Figure 2 reports the plot of the polar curves computed at the design Mach. The pressure dis-

Presented as Paper 94-1896 at the AIAA 12th Applied Aerodynamics Conference, Colorado Springs, CO, June 20–23, 1994; received Sept. 22, 1994; revision received Jan. 7, 1995; accepted for publication Jan. 7, 1995.

*Research Engineer, Transport Aircraft Aerodynamics Group, Via Maiorise.
†Physics Graduate, IRSIP—Istituto Ricerche Sistemi Informatici Paralleli, Via P. Castellino 111.

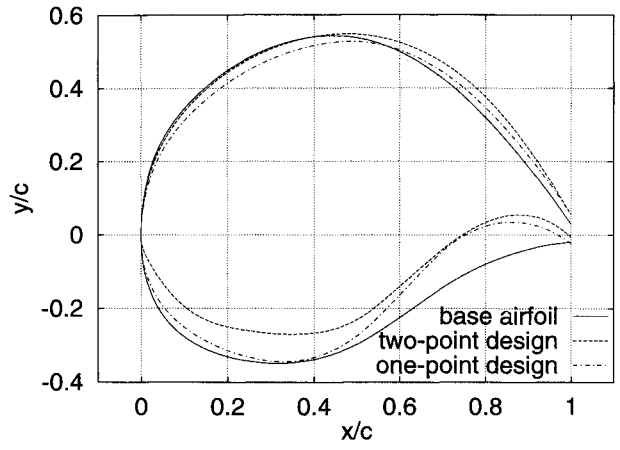

Fig. 1 Base and final airfoils.

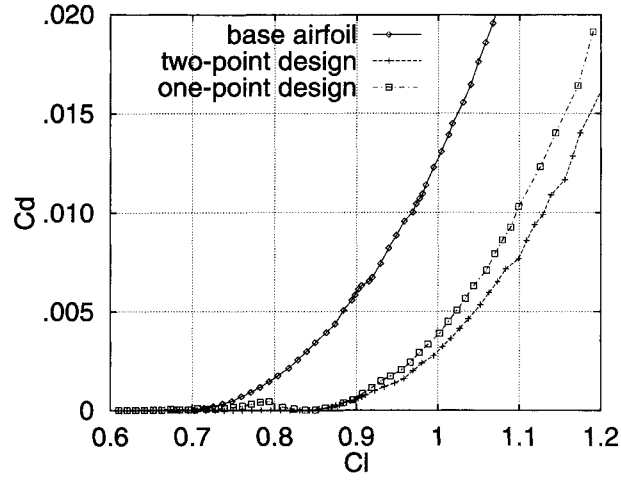

Fig. 2 Polar curves at $M = 0.745$.

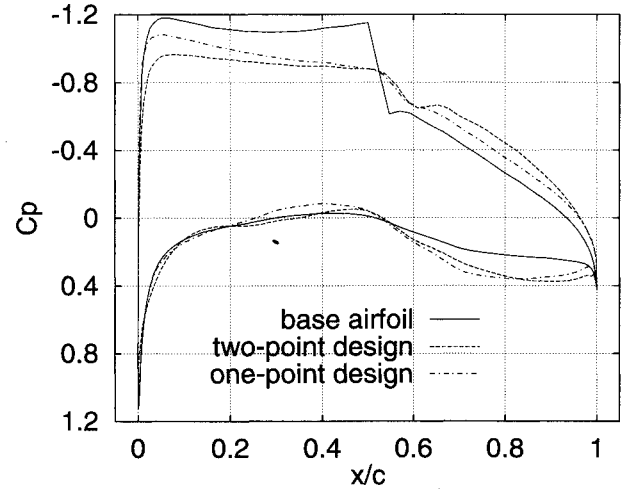

Fig. 3 Pressure distributions at the design point $M = 0.745$, $Cl = 0.855$.

tributions on the base and final airfoils at the design point are shown in Fig. 3.

Two-Point Design

The previous results are characterized by good behavior at the design point, but they present poor results for lift coefficients that are a little lower than the fixed one. In particular, the inviscid computation shows the appearance of an undesired double compression.

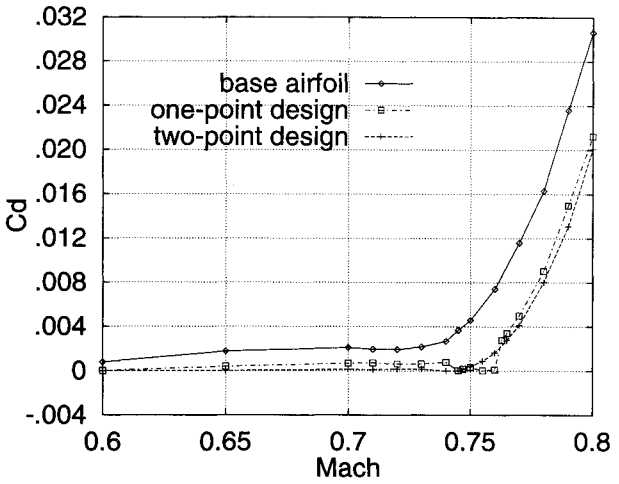

Fig. 4 Wave drag evaluation at off-design conditions.

In order to avoid this, a two-operating condition design problem has been set up. The first one is equal to the previous one, while the second one was chosen at $Cl_2 = 0.755$ and $M = M_1 = M_2$, where the first solution failed. The objective function then becomes

$$\max \frac{1}{(Cd_{w_1}/Cl_1^2) + (Cd_{w_2}/Cl_2^2)} \tag{4}$$

The results related to this computation are reported in previously mentioned Figs. 1–3, where they can be directly compared with the single-point case.

Here, it can be observed that the number of generations needed to reach a good solution is much greater than in the previous cases. After 490 generations, the fitness reached a satisfactory value and the computation was continued until the 566th generation was reached. The statistics related to this run are 15,878 airfoils analyzed; 6543 discarded; 3723 evaluated using the flowfield solver; score assigned to the remaining 5610 airfoils without computation.

Finally, Fig. 4 is related to the off-design performance of the airfoils.

Conclusions

In the present work a transonic airfoil design system, based on a genetic algorithm, has been presented. The optimization procedure was tested both on a one-operating condition design problem and a two-operating condition one. The obtained results show that the genetic algorithm developed is able to achieve satisfactory designs of shockless airfoils.

References

[1]Tong, S. S., Powell, D., and Skolnick, M., "EnGENEous: Domain Independent, Machine Learning for Design Optimization," *Proceedings of the 3rd International Conference on Genetic Algorithms*, edited by J. D. Schaffer, M. Kaufmann Publishers, San Mateo, CA, 1989, pp. 151–159.

[2]Hajela, P., "Genetic Search—An Approach to the Nonconvex Optimization Problem," *AIAA Journal*, Vol. 28, No. 7, 1990, pp. 1205–1210.

[3]Mosetti, G., and Poloni, C., "Aerodynamic Shape Optimization by Means of a Genetic Algorithm," *Proceedings of the 5th International Symposium on Computational Fluid Dynamics*, Vol. 2, Japan Society of Computational Fluid Dynamics, Tokyo, Japan, 1993, pp. 279–284.

[4]Goldberg, D. E., "Genetic Algorithms in Search, Optimization and Machine Learning," Addison–Wesley, Reading, MA, 1989.

[5]Holland, J. H., *Adaptation in Natural and Artificial Systems*, Univ. of Michigan Press, Ann Arbor, MI, 1975.

[6]Ghielmi, L. G., Marazzi, R., and Baron, A., "A Tool for Automatic Design of Airfoils in Different Operating Conditions," AGARD CP-463, Loen, Norway, 1989.

Dihedral for Spiral Stability

Amnon Katz*
University of Alabama,
Tuscaloosa, Alabama 35487-0280

Nomenclature

a = airframe acceleration
b = wingspan
C_{Lw} = lift coefficient of the wing
c = wing chord
c_l = lift coefficient of a wing section, two dimensional
g = magnitude of the acceleration of gravity
l_f = moment arm of the fin (vertical tail)
M = moment
S = wing area
V = airframe velocity, relative to the air mass
x = body coordinate positive forward
y = body coordinate positive to the right
z = body coordinate positive down
α_f = angle of attack of the fin (vertical tail)
α_w = wing angle of attack
α_{w0} = zero lift angle of attack of the wing
α_{w1} = modified angle of attack of the wing
β = angle of sideslip
Γ = wing dihedral angle
Γ_0 = wing dihedral angle for neutral spiral stability
η = dimensionless spanwise variable, $2y/b$
ϕ = bank angle
ω = angular velocity

I. Introduction

THIS Note sets forth a rule of thumb to determine the wing dihedral angle that assures lateral stability in a low-speed airframe. The amount of dihedral Γ_0 that corresponds to neutral stability against the spiral mode is related to the wing angle of attack, measured from zero lift, and to the ratio of wingspan to fin moment arm:

$$\Gamma_0 = \kappa(b/l_f)(\alpha_w - \alpha_{w0}) \tag{1}$$

Section II offers an approximate, "back of the envelope" derivation of (1), assuming a rectangular spanwise lift distribution. Section III compares the predicted Γ_0 to data obtained from a full six degrees-of-freedom dynamic computer simulation. Section IV refines the analysis to address a general lift distribution. The value of κ in (1) depends on the shape of the distribution. Sample values are

$$\kappa = \begin{cases} \frac{2}{3} \approx 0.67 \text{ (rectangular)} \\ 3\pi/16 \approx 0.59 \text{ (elliptic)} \\ \frac{1}{2} = 0.50 \text{ (triangular)} \end{cases} \tag{2}$$

Received Aug. 10, 1994; revision received Nov. 28, 1994; accepted for publication Dec. 15, 1994.

*Professor, Department of Aerospace Engineering, P.O. Box 870280. Member AIAA.

II. Rudimentary Analysis

A forward, right, down body system of coordinates is used throughout. Components of vectors are in the body system and are denoted by subscripts x, y, z.

When an airplane is banked at an angle ϕ, gravity produces a lateral acceleration

$$a_y = g \sin\phi \tag{3}$$

This causes the trajectory to curve. The fin (vertical tail), acting as a weathervane, forces the airplane to turn and remain approximately aligned with the curved trajectory. The rate of turn is

$$\omega_z = a_y/V = (g/V)\sin\phi \tag{4}$$

The yaw rate creates an asymmetrical flow over the airframe. The wing on the outside of the turn travels faster than the wing on the inside, creating more lift, and therefore, a rolling moment into the turn, hence, spiral instability.

The local velocity along the wing is $V + \omega_z y$. The first-order rolling moment that results is

$$M_{1x} = \rho V \omega_z \int_{-(b/2)}^{b/2} c_l c y^2 \, dy \tag{5}$$

Assume a rectangular lift distribution

$$c_l c = C_{Lw} S/b \tag{6}$$

where C_{Lw} is the lift coefficient of the wing. When (6) is substituted in (5), one finds

$$M_{1x} = \tfrac{1}{12} C_{Lw} \rho S V \omega_z b^2 \tag{7}$$

Converted to a moment coefficient (normalized to the volume bS) this becomes

$$C_{M1x} = C_{Lw}(b\omega_z/6V) = C_{Lw}(bg/6V^2)\sin\phi \tag{8}$$

This rolling moment tends to increase the bank. To insure spiral stability, it must be canceled and reversed by some other rolling moment.

The asymmetrical flow also creates yawing tendencies. One way that this arises is through increased drag on the outside wing, which tends to yaw the nose of the airplane to the outside of the turn. This effect may be calculated similarly to Eq. (5), but with lift replaced by drag. The effect is much smaller because wing drag is much smaller than wing lift. We will neglect this contribution.

A more significant effect is produced by the fin. The yawing creates a side flow at the fin in the amount of $\omega_z l_f$. Given this lateral flow and any sideslip angle β that may exist, the angle of attack of the fin becomes

$$\alpha_f = \beta - (l_f \omega_z/V) \tag{9}$$

The weathervane effect forces this angle of attack to zero, creating a sideslip angle

$$\beta = l_f \omega_z/V = (l_f g/V^2)\sin\phi \tag{10}$$

The banked and turning airplane, left to its own devices, points towards the outside of the turn. This is a well-known secondary effect. Pilots performing a steady turn compensate by applying rudder into the turn. They also neutralize the moment (5) by applying aileron against the turn.

The passive, controls fixed, airframe actually maintains a sideslip angle while it turns. This is where the effect of dihedral comes in. A dihedral angle Γ combined with a sideslip angle